



Review

Co-Torrefaction Progress of Biomass Residue/Waste Obtained for High-Value Bio-Solid Products

Abdul Waheed ¹, Salman Raza Naqvi ^{1,*}  and Imtiaz Ali ² 

¹ Laboratory of Alternative Fuels & Sustainability, School of Chemical and Materials Engineering (SCME), National University of Science and Technology, H-12, Islamabad 44000, Pakistan

² Department of Chemical and Materials Engineering, King Abdulaziz University, Rabigh 21911, Saudi Arabia

* Correspondence: salman.raza@scme.nust.edu.pk; Tel.: +92-333-3754488

Abstract: The co-torrefaction of several biomasses may be a viable solution in the study area, as it produces biofuels and addresses waste-treatment concerns. This review evaluates biomass through ultimate, proximate, and FTIR analyses, and the mechanism of the co-torrefaction process is observed for product quality with a synergistic effect. Furthermore, the parameters of co-torrefaction, including temperature, reaction time, mass yield, energy yield, and the composition of the H/C and O/C ratio of the co-torrefied materials, are similar to those for coal composition. Different reactor types, such as fixed-bed, fluidized-bed, microwave, and batch reactors, are used for co-torrefaction, in which biomass blends with optimized blend ratios. The co-torrefaction process increases the bio-solid yield and heating value, the capacity to adsorb carbon dioxide, and the renewable fuel used for gasification. One of the objectives of this study is to adopt a process that must be viable, green, and sustainable without generating pollution. For this reason, microwave co-torrefaction (MCT) has been used in many recent studies to transform waste and biomass materials into an alternative fuel using a microwave reactor.

Keywords: co-torrefaction; reactors; bioenergy; biomass; bio-solid; bio-oil; bio-gas



Citation: Waheed, A.; Naqvi, S.R.; Ali, I. Co-Torrefaction Progress of Biomass Residue/Waste Obtained for High-Value Bio-Solid Products. *Energies* **2022**, *15*, 8297. <https://doi.org/10.3390/en15218297>

Academic Editor: Antonio Galvagno

Received: 18 September 2022

Accepted: 1 November 2022

Published: 7 November 2022

Publisher's Note: MDPI stays neutral with regard to jurisdictional claims in published maps and institutional affiliations.



Copyright: © 2022 by the authors. Licensee MDPI, Basel, Switzerland. This article is an open access article distributed under the terms and conditions of the Creative Commons Attribution (CC BY) license (<https://creativecommons.org/licenses/by/4.0/>).

1. Introduction

Since the beginning of the industrial era in the 18th century, the world has consumed most of the fossil fuels (such as coal, oil, and natural gas) at a high speed [1]. The widespread use of fossil fuels has led to two major crises: energy depletion and global warming. As a result, the development of renewable energy and the reduction in carbon dioxide emissions have become a critical priority in the 21st century [2,3]. People in various countries depend on biomass as a sustainable energy source to meet the expanding energy demands and support economic growth [4,5]. Most biomasses have a low carbon content and high oxygen, hydrogen, and sulfur contents, which maximizes air pollution and greenhouse gas emissions [6,7]. In the opinion of most experts, the development of renewable energy, at present, is essential to reduce the use of fossil fuels, greenhouse gas emissions, and ecological pollution. Renewable biomass or bioenergy is the most abundant energy source in technologies to date [8–11].

Various categories of biomass resources are processed using various thermochemical techniques, such as torrefaction and pyrolysis, including gasification, which uses higher temperatures (≥ 200 °C) to valorize biomass into bio-solids and bio-oil, including syngas [10,12,13]. Renewable energy generated from wind, solar, hydro, geothermal, and biomass [14,15] sources is replacing energy derived from fossil fuels. Bioenergy derived from biomass has some potential to partially replace non-renewable sources, such as coal (electricity generation). However, compared to coal, biomass, by nature, has a lower energy density, greater moisture levels, and volatiles [16]. Due to this, biomass must undergo pre-treatment to enhance its qualities before it can be used instead of fossil fuel [17]. Pyrolysis, which depends on temperature and heating rate, promotes the synthesis of bio-solid,

bio-oil, and syngas from biomass resources in an inert environment [18,19]. Torrefaction uses moderate temperatures (200–300 °C) to convert biomass into fuel bio-solids [20–22]. Co-torrefaction is the heating of two biomasses at 200–300 °C in an inert environment. Due to the higher biomass-to-coal ratio, fuel has greater flexibility and produces less tar [23,24].

Several previous studies emphasized co-thermal processing, such as the co-pyrolysis of waste resins and conventional biomass, and also reported their interaction effects. For example, the synergistic impact on liquid and gas yields was identified when biomass was combined [25]. As a result of the addition of pine cones to polymeric materials, the number of gaseous products increased more than expected, resulting in a lower char yield [26]. Co-torrefaction is feasible for the production of bio-solids [27]. The bio-solid fuels can be utilized for co-firing or environmental remediation applications through the thermochemical process (torrefaction) [28]. The use of biomass for co-torrefaction with a low calorific value implies the maximum amount of oxygen and hydrogen in the biomass. Co-torrefaction can increase the calorific value of a bio-solid fuel by removing the moisture content and the decomposing part of the volatile matter [29]. Microwave co-torrefaction of an empty fruit bunch with used engine oil at 300 °C has been shown to improve the high heating value (28.0 MJ/kg) of solid fuel [30]. Numerous types of biomass waste can be used without harming the environment [31]. Solid biomass and bio-oil can be combined by mixing several biomass ratios, thus reducing waste disposal and greenhouse gas emissions [32–34]. The co-torrefaction of various feedstocks improves the fuel properties of the product [35]. It is challenging to store hygroscopic raw biomass because of its higher moisture content and lower energy density [36,37]. This means that the use of raw biomass as a fossil fuel alternative, such as coal, is limited because of these features. Processing, on the other hand, can address the drawbacks of raw biomass. To achieve this, biomass can be pretreated by a process known as co-torrefaction. Temperatures of 200 °C–300 °C are used under vacuum, and nitrogen is supplied during the heating of raw biomass [22,36]. Furthermore, the study observed that co-torrefaction can significantly increase the properties of biomass at some levels [38], such as reducing the moisture content of the raw biomass, resulting in higher energy density and a higher heating value (HHV) [39]. Furthermore, the hygroscopic characteristic of raw biomass has been transformed into hydrophobic fuel [40]. Figure 1a presents the total publications obtained from different countries, while Figure 1b indicates the dynamics of the yearly publications.

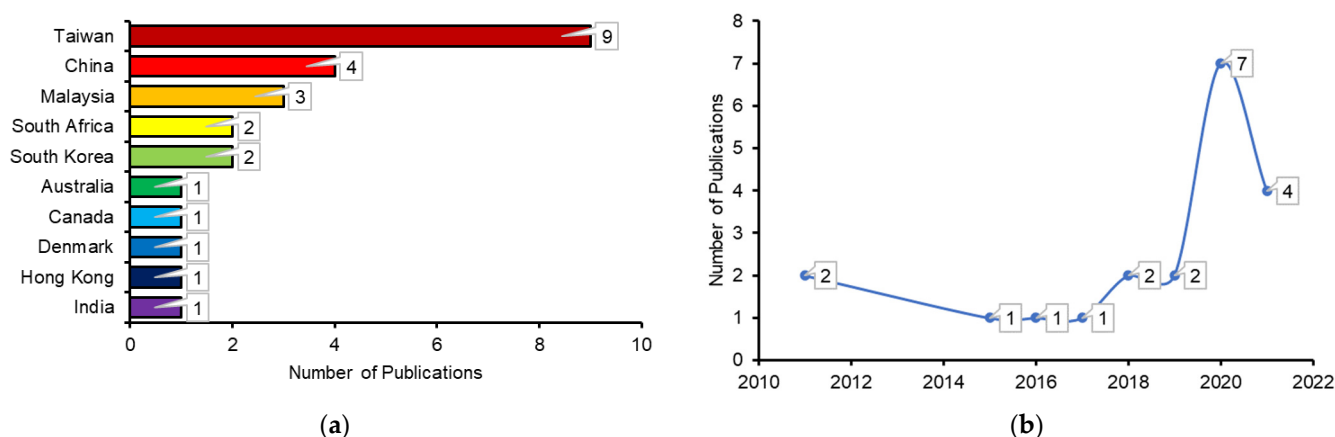


Figure 1. Number of publications in the co-torrefaction process (a) country-wise for the whole period and (b) year-wise retrieved from the Scopus database (2 October 2022).

The following table summarizes the most recent research conducted on the co-torrefaction of biomass and garbage, including studies, features, and outcomes. The co-torrefaction of biomass as feedstock did not indicate a synergetic effect. The torrefied product presented an inconsequential improvement in HHV for use as a fuel co-fire [41]. The co-torrefaction process used empty fruit bunch (EFB) pellets as the primary feedstock and cooking oil

(UCO) as the secondary feedstock to enhance the calorific value, and hence the increased quality of the EFB pellets. As a result, high-calorific-value torrefied pellets that are more environmentally friendly were produced. Microwave co-torrefaction (MCT) is a new technology that combines microwave heating with co-torrefaction [42]. Torrefied biomass pellets were compared with typical furnace-based co-torrefaction in terms of their properties, manufacturing process, waste reduction, and energy-conversion efficiency [42]. A torrefied biomass can be integrated into coal-fired boilers through direct, indirect, or simultaneous co-firing systems [43]. The study shows that microwave heating is an innovative technology integrated with the torrefaction process [42,44]. The work conducted on the co-torrefaction of various biomass and waste materials is summarized in Table 1.

Table 1. Latest developments in the co-torrefaction process.

Sr. No.	Biomass Type	Blending Ratio	Process and Type of Reactor	Process Condition	Outcome	Application	Ref.
1	Waste epoxy resin and fir	Mixing ratio of fir:waste epoxy resin is 1:3	Co-torrefaction Conventional heating batch-type reactor	Temperature: 120 °C–180 °C, time: 10 min–40 min	Solid yield 76.86%. Enhancement in HHV 1.12 Energy yield 85.79% Improved evaporation of volatile compounds. Solid yield adversely affected	Improvement of biochar	[23]
2	Sewage sludge and Leucaena	Mixing ratio of sewage sludge:Leucaena is (75:25%)	Co-torrefaction Microwave heating	Microwave power level 100 W, time: 30 min, temperature: 170 °C–390 °C	Bio-char made from pure Leucaena wood has a CO ₂ adsorption capacity of 53 mg/g	Solves waste-water problem. Production of biofuels	[44]
3	Biomass and coal	Blending ratio of biomass:coal is (30:70%)	Vertical tubular furnace	Temperature: 300 °C, time: 60 min	Produced mass yield: (57.0–63.8%), energy yield: (77.0–89.0%), (18.1–22.2%) reduction in CO ₂ emissions Better temperatures (92.6%) result in higher energy efficiency, but the moisture content of the feed mixture quickly decreases this efficiency (16.9 to 57.3% for 70% moisture)	Enhances the quality of coal	[45]
4	Microalgae and Lignocellulosic biomass	-	Co-torrefaction A gas chromatographic furnace with a glass reactor	Temperature: 250 °C, time: 60 min	Higher heating value of 19.0 MJ/kg, 92.1% of energy yield, fuel ratios of 1.60–1.82, and an energy return on investment of 14.7% HHV:19.6 MJ/kg; decreased ash content; first-order kinetics; increased thermal stability and combustion efficiency of biochar; 7.4 energy return on investment; 45.2% reduction in carbon gas emissions	High production of bio-char with high calorific value	[35]
5	Mango seed and passion shell with optoelectronic sludge	Blending optoelectronic sludge with mango seed in a 25/75 ratio	Wet co-torrefaction Microwave reactor	Temperature from 120 °C to 180 °C, reaction duration from 10–40 min	There is an 85.5 wt% mass yield Fuel ratio: 1.8. Carbon content: 68.3%. Fixed carbon: 62.3%. HHV: 28.0 MJ/kg.	The production of fuel of the highest grade	[46]
6	Food sludge and lignocellulosic biowaste	Mixing macadamia husk and sludge in a (25/75%) ratio (db%)	Wet co-torrefaction Microwave reactor	Temperature: 150 °C, duration: 20 min	There is no synergistic effect of co-torrefaction on weight loss of the blend	Production of bio-solid and nutrient recovery	[41]
7	Empty fruit bunch pellet, used cooking oil, and waste engine oil	-	Co-torrefaction Microwave reactor	Temperature: 200, 250 °C and 300 °C, heating rate: 50–65 °C/min, time: 5–8 min	Amount of fixed carbon: 29.8%, HHV: 19.7 MJ/kg	Production of solid fuel with greater improvement	[30]
10	Hemicellulose, cellulose, lignin, xylan, dextran, xylose, and glucose Textile sludge and lignocellulose biowaste	Weight ratio (1:1:1)	Co-torrefaction Conventional heating thermogravimetry	Temperature: 230 °C, 260 °C and 290 °C	Production of biofuel	-	[47]
11	(macadamia husk) Mango branches (MBr), waste newspaper (Np), and low-density polyethylene (LDPE)	-	Wet co-torrefaction	Temperature: 120 °C–180 °C, time: 10–30 min	Improved fuel characteristics that allow co-firing		[41]
12	Food sludge and six widely produced lignocellulose bi-wastes	Three binary mixtures prepared, with a mass ratio of 1:1	Bench-scale tubular reactor	Temperature: 300 °C	(MBr-LDPE) carbon content: 71.94% HHV: 35.84 MJ/kg		[48]
13		Blending ratios of 0/100, 25/75, 50/50, and 100/0	Microwave heating system	Torrefaction temperature (120, 150, and 180 °C), reaction time (10, 20, and 30 min)	Food sludge blended with macadamia husk (25/75 db%) highest fixed carbon content (25%) HHV: (19.6 MJ/kg)	Renewable energy resource.	[41]

This article presents the detailed information about the co-torrefaction process and its mechanisms. It also explores the role of temperature and residence time on higher heating value (HHV), mass, and energy yield during the co-torrefaction process. The main idea in

this paper is the Ven Krevelen diagram used to describe the quality of co-torrefied biomass. Process variables, reactor type, and numerous analysis tools are presented, including proximate and ultimate analyses. The impacts of mixing ratios and thermogravimetric measurements of mixing biomass are also discussed. Furthermore, numerous reactor configurations and applications for co-torrefaction processes are studied.

2. Biomass Residue and Their Analysis

2.1. Ultimate Analysis

The ultimate analysis presents the compositional analysis in its constituent elements, such as (carbon, oxygen, hydrogen, nitrogen, and sulfur). The carbon content of bio-waste is vital for increasing the value of HHV and decreasing CO_x emissions in the environment. The characteristic of biofuels improves with a decrease in oxygen content, increasing stability, and reducing the production of smoke (e.g., light material) through combustion [49]. The oxygen, sulfur, and nitrogen content of optoelectronic sludge (OS) and bio-waste decreased. In contrast, the carbon content increased as a result of the co-torrefaction process. Nitrogen (6.4 wt.%) and sulfur (4.6 wt.%) were deficient in the raw and torrefied products, leading to lower sulfur and nitrogen oxide emissions during burning. The co-torrefaction of OS and bio-waste increased the release of hydrophilic functional groups, thus dehydrating bio-solids as presented in Table 2 [46]. Furthermore, during wet co-torrefaction, deoxygenation and decarboxylation reactions occurred [50]. Excess lignocellulosic material is expected to degrade during the torrefaction of EFB pellets, resulting in incondensable bio-oil and incondensable syngas [42]. Increasing the temperature to 300 °C resulted in a higher degree of devolatilization, resulting in the higher carbon content of torrefied biomass pellets. [42]. The atomic ratio of hydrogen, oxygen, and carbon helped us to understand the heating value of the fuel. The heating value of the co-torrefied product depends on the oxygen-to-carbon ratio (O/C) and is very important, as the heating value decreases from 18.90 to 13.57 MJ/kg with an increase from 0.99 to 1.02, as presented in Table 2. With the mix of OS and MIse (25/75%) with a temperature of 150 °C at 30 min, the value of (O/C) decreased to 0.88 with an increase in HHV to 19 MJ/kg [46]. Another major factor affecting the heating value is the hydrogen-to-carbon (H/C)-ratio value. The HHV of biomass was 14.8 MJ/kg for 0% lignocellulosic material (Lc) with a value (H/C) of 0.12, and the HHV for 100% Lc was 21.4 MJ/kg with a value (H/C) of 0.07, the lowest and highest values, respectively. Mixtures for co-torrefaction with Lc included at 0% to 50% achieved HHVs greater than 18 MJ/kg at a temperature of 300 °C, as concluded from Table 2 [35]. Additionally, the elimination of nitrogen and deoxygenation reactions had a substantial impact on the final qualities of the bio-char content; therefore, bio-solids that experienced a co-torrefaction process at temperatures higher than 275 °C were shown to have improved fuel properties [51].

Table 2. Ultimate and proximate analyses of torrefied biomass.

Biomass/Torrefied Biomass	Temp (°C)	Time (min)	Carbon (%)	Hydrogen (%)	Nitrogen (%)	Oxygen (%)	Sulphur (%)	Moisture (%)	Volatile Matter (%)	Fixed Carbon (%)	Ash (%)	HHV (MJ/kg)	Ref.
OS	–	–	43.89	4.80	6.38	43.48	1.45	99.00	64.89	9.30	25.81	13.57	[46]
Mangifera indica seed (MIse)	–	–	46.11	5.54	0.89	47.20	0.27	4.97	96.38	2.24	1.38	18.90	[46]
OS and MIse (25/75%)	150	30	45.1	9.8	4.6	39.6	0.9	–	–	–	3.0	19.0	[46]
EFB	–	–	43	6	1.2	49.8	0	15	62	15	8	18.5	[42]
EFB pellet with UCO	300	–	68.2	8.0	0.7	23.1	0	1	33	63	3	26.4	[42]
Cv	–	–	51.29 ± 0.09	7.31 ± 0.42	9.05 ± 0.00	32.11 ± 0.10	0.24 ± 0.04	6.35 ± 0.52	86.46 ± 0.74	6.01 ± 0.73	7.53 ± 0.09	15.54	[35]
Lc	–	–	50.10 ± 0.16	6.21 ± 0.09	1.10 ± 0.08	42.59 ± 0.04	0.00 ± 0.00	9.28 ± 0.84	78.41 ± 3.89	19.06 ± 3.97	2.53 ± 0.08	18.94	[35]
Lc 100%	300	45	70.2	5.1	1.5	21.9	1.2	5	58.6	34.9	6.5	21.4	[35]
Lc 50%	300	30	61.2	6.0	5	27.6	0.2	30	63.0	26.6	10.5	19.1	[35]

2.2. Proximate Analysis

Proximate analysis bases its estimates on moisture, volatile matter (VM), fixed carbon (FC), and ash [52]. The reduced VM and ash content increased the energy density of the pellets and improved the stability of the flame following the pre-treatment of the biomass (co-torrefaction) [42]. Bio-oil and incondensable syngas are projected to emerge from

the decomposition of the lignocellulosic component of EFB pellets during torrefaction, while the FC and carbon content of subsequent torrefied biomass pellets increases [53]. A temperature of about 300 °C resulted in a higher degree of devolatilization, resulting in a higher carbon content in torrefied biomass pellets [27].

The proximate compositions of bio-char were estimated and their HHV values utilized to establish their potential for energy or material applications. Initially, the moisture content of EFB was 15% and HHV was 18.5 MJ/kg. The moisture level of the EFB pellets containing the used cooking oil was equal to 1, and the HHV increased to 26.4 MJ/kg, which was substantially higher than EFB alone, as determined in Table 2 [42]. The proximate compositions of the *Chlorella vulgaris* (Cv) and Lc samples differed significantly. Cv had more ash with a value of 7.53%, while Lc included more fixed carbon at 19.06%. Lc-reduced ash at 2.53% is associated with a greater HHV due to energy recovery and also the low Cv value associated with the fixed carbon value of 6.01%, as presented in Table 2 [35]. Hybrid coal has a low moisture content and a narrow range of 0.6–2.1% by *w/w* [45,54]. Bio-solid acquires its hydrophobic properties by dehydration, which also prohibits the generation of hydrogen bonds [51].

Furthermore, the heat obtained from the feed evaporated the moisture at approximately 108 °C, accompanied by the evaporation of volatile compounds at temperatures higher than 200 °C [45]. During torrefaction, the biomass constituent, mainly hemicellulose, decomposes and becomes free of volatile matter [17]. Due to this, the VM content of the hybrid coal is reduced while its FC content increases. Regarding VM, sugarcane bagasse biomass is the most effective, followed by rubberwood and empty palm fruit bunches [45]. Lc 50% at a temperature of 300 °C had a VM of 63% with a HHV of 19.1 MJ/kg, and in Lc 100%, the VM was 58.6% with a temperature of 300 °C with a HHV of 21.4 MJ/kg, as presented in Table 2. This shows that the impact of an increased VM value decreased the energy density of the biomass. During the torrefaction process, the ash remained fixed, which caused this effect [55]. The variations in the ultimate and proximate analyses of biomass before and after co-torrefaction are presented in Table 2.

2.3. FTIR Analysis

The microscopic chemical composition can be deduced from FTIR [56] analysis. Xyloglucan, xylan, and glucomannans may all be present in hemicellulose [57]. This technique exposes the structural makeup of hemicellulose [54]. For example, FTIR was also used to analyze the conversion of cellulose, which is the main component of plant cell walls [56]. FTIR is an efficient method used for studying hydrogen-bond formation in amorphous cellulose [58]. Furthermore, numerous lignin compounds based on the differences in hydrogen-bonding mechanisms between hardwood and softwood are also determined using this technique [59]. In one study, the cellulose in the raw MIse and PEsh samples was associated with peaks at 910–945 cm^{-1} and 1110 cm^{-1} , respectively; the lignin in these samples was associated with peaks at 1213, 1427, and 1506, and the hemicellulose fraction was associated with peaks at 1063, 1244, and 17,440 cm^{-1} [60,61]. The deoxygenation, dehydration, and decarboxylation of the co-torrefied samples led to the destruction of cellulose, hemicellulose, and lignin in biochar, as can be observed by the much lower peak intensities of the co-torrefied samples compared to the raw samples (i.e., OS, MIse, and PEsh) presented in Figure 2 [46].

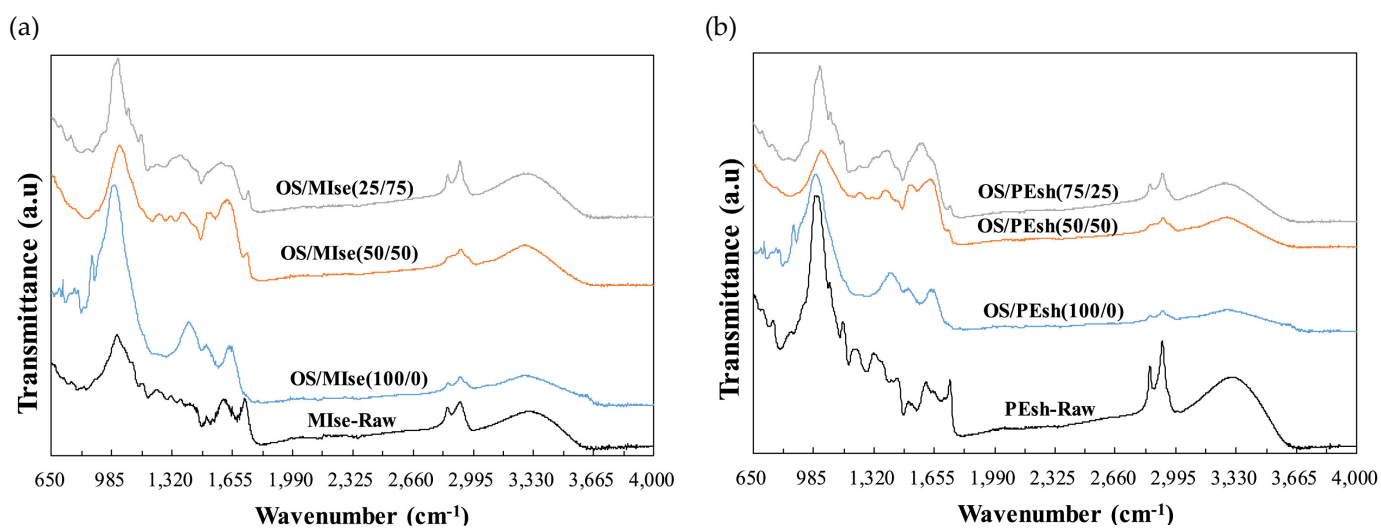


Figure 2. (a) Raw MlSe and co-torrefied OS/MlSe with different blended ratios; (b) raw PEsh and co-torrefied OS/PEsh with different blended ratios. Reprinted with permission from Ref. [46]. Copyright © 2021 Elsevier Ltd.

3. Co-Torrefaction Mechanism and Operation Parameters

3.1. Co-Torrefaction Process

Co-torrefaction occurs when two biomass blends undergo a process and are converted into a bio-solid. Figure 3 illustrates the process of co-torrefaction. In Figure 3, two residual/waste biomass were blended together in various blending ratios (0:100, 25:75, and 50:50%). The feedstock was placed into the furnace for pre-treatment (co-torrefaction) and run under vacuum with a supply of nitrogen, so that an inert atmosphere was created in the furnace in order to avoid the possible ignition of the sample. The duration of this step depended on the flow rate and size of the furnace. After purging the supply of nitrogen was interrupted, the sample was kept in a crucible placed in the central furnace with a heating rate of 10 °C/min in the temperature range of 200–300 °C for a residence time of 30 min to 2 h [62]. Three products (bio-oil, bio-solid, and bio-gas) were obtained from the furnace following the co-torrefaction of blending the residual biomass. The main outcome of the co-torrefaction process is a high-quality bio-solid product [63]. The co-torrefaction process is endothermic at low temperatures, but progresses toward an exothermic process when char is formed during the thermal degradation of lignocellulosic biomass at high temperatures [64]. During the degradation of the components, various reactions are involved. The first stage is to remove the moisture content at 110 °C. The following stage is to remove inbound moisture or a fully moisture-free environment when the temperature increases to 200 °C. At 200 °C, the torrefaction process begins to decompose volatile matter to produce solid, liquid, and gaseous products. At 200–250 °C, the stage of decomposition of hemicellulose occurs that is characterized by limited devolatilization, and a solid structure is formed. During this stage, C-C, C-O, and inter- and intramolecular hydrogen breakdowns occur, which form condensable liquids and non-condensable gases. The stage of 250–300 °C is the extensive part of the torrefaction process in which hemicellulose decomposes into volatiles and solid products are formed [42].

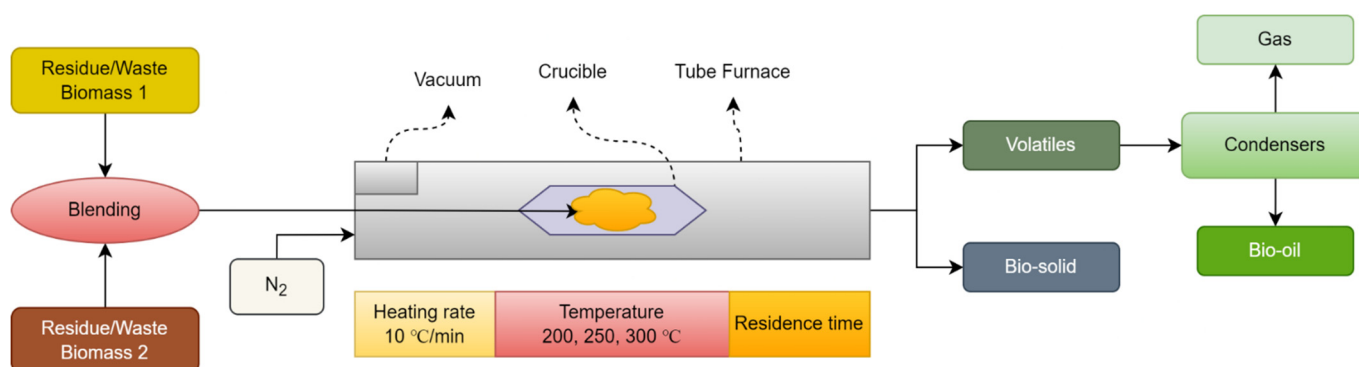


Figure 3. Co-torrefaction process.

3.2. Synergistic Effect

When two or more biomass wastes combine to generate a more significant impact than either of them could produce alone, this is called a synergistic effect. When materials are combined, synergistic effects may be used to increase co-torrefaction yields. Furthermore, the combination of OS with MIse and *Passiflora edulis* shell (PEsh) for wet torrefaction (WT) has a synergistic impact on the increase in HHV content in co-torrefied bio-solid, especially in a 75/25% ratio [46]. As a consequence of these results, combining OS with fruit bio-waste is an additional effective way to help the process, involving the betterment of the bio-solid as a product. Therefore, it is likely to be used instead of traditional fuels in the future (e.g., coal) [65].

3.3. Operating Parameters

The co-torrefaction process utilized a variety of biomasses that were thermochemically processed and acquired desirable qualities. During the co-torrefaction of biomass, numerous operating parameters affected the co-torrefaction process, such as the role of temperature, residence duration on mass and energy yields, and the HHV of biomass, and the Van Krevelen diagram.

3.3.1. Studying the Role of Temperature and Residence Time on Mass and Energy Yields

The mass and energy yields of the co-torrefied biomass varied with temperature and the reaction time. The increase in temperature and residence time decreased the mass and energy yields, while the energy density increased. The mass yield of OS decreased when the co-torrefaction temperature increased from 120 °C to 180 °C, from 98.4% after 10 min at 150 °C to 79.9% after 30 min at 180 °C. The main constituents of raw sewage (such as low-molecular-weight hydrocarbons) were degraded with the increasing co-torrefaction intensity. This reaction had an energy density of 1.14 and a 100% energy yield at 150 °C for a reaction time of 30 min [46]. During co-torrefaction at a temperature of 150 °C and a reaction time of 10 min, a further 99.4% energy yield was obtained with an associated energy density of 1.01 [46]. As a result, unnecessary energy consumption is reduced, and a high HHV of bio-solid is obtained [46]. During 20 min of torrefaction at 150 °C, 95.2% of the energy was extracted, with a maximum energy density of 1.20.

The mass and energy yields were affected by various blend ratios and types of biowaste used [29]. The OS and bio-waste co-torrefied together produced more than 80% of the total mass and energy yield. These were the same yields reported for the microwave-based torrefaction of OS, which may have been due to the heating of the samples from the inside at lower temperatures and for shorter periods, leading to their higher energy efficiency [66]. This might be because microwave-irradiation heating modes are more energy efficient, as they can heat the interiors of materials at lower co-torrefaction temperatures for shorter periods of time [67]. The bulk bio-solid yields decreased when the ratio of the OS/biowaste blend was reduced from 75/25 to 25/75%, especially in the case of the PEsh OS blend [46]. This phenomenon occurs because biomass has a higher microwave-absorption capacity

than sludge, resulting in the considerable devolatilization of biomass as the percentage of bio-waste in the mix increases [68]. Because MIse and PEsh have lower energy densities than those of pure OS, they increase the energy density of pure OS. When OS is combined with MIse and PEsh bio-wastes, the energy and mass yields are the same. When the OS/bio-waste blending ratio was altered from 75/25% to 25/75%, the bio-solid mass yields decreased from 95.1% to 92.1% for OS combined with MIse and 93.4–65.2% for OS mixed with PEsh. These results are consistent with the other research investigating the co-torrefaction of sewage sludge and *Leucaena* using microwave heating [67]. Note that when the OS–PEsh and OS–MIse co-torrefied bio-char was mixed at 50/50 and 25/75%, the mass recovery and energy yields of the OS–PEsh co-torrefied bio-solid were substantially lower than those of the OS–MIse co-torrefied bio-solid [46]. Furthermore, when bio-waste and sludge are mixed for co-torrefaction, heat can degrade a significant amount of hemicellulose and cellulose, reducing the mass and energy yields of bio-char while maintaining its higher energy content [68]. Furthermore, bio-solids produced from co-torrefied food waste offer an improved substitute for peat in terms of their thermal qualities when combined with sugarcane bagasse, rice straw, *Pisidium guajava*, *Annona squamosa*, macadamia husk, and pistachio husk, respectively [41].

3.3.2. Studying the Role of Temperature and Residence Time on HHV

The quality of a bio-solid can be significantly influenced by the proportions of biomass used in the mixing process. The combination of OS with MIse and PEsh bio-waste generates a bio-solid with different HHVs. The MIse and PEsh biowastes were observed to have experimental HHVs of 19.4 and 18.6 MJ/kg, respectively, which was significantly higher than OS (15.5 MJ/kg) after 30 min of torrefaction at 150 °C; microwave-assisted WT was used to mix textile sludge and lignocellulose bio-waste, and bio-char HHV increased in the same proportion as the blending ratios of the two types of bio-waste increased. Following 30 min of torrefaction at 150 °C, it was revealed that the maximum high-heating values of OS mixed with MIse and PEsh were better than those obtained with the other blending ratios (75/25 and 50/50%). These were 19.0 and 18.3 MJ/kg, respectively [46]. The resulting bio-solid had a maximum of 19.2–21.1 MJ/kg HHV, which was an increase over lignite coal (19.2–21.1 MJ/kg) [69]. A total of 55% of the carbon in bio-char was fixed carbon compared to raw food sludge (FS). The fixed carbon and ash contents of biomass increased when the FS and bio-waste were mixed. As a result, agricultural bio-waste can be appropriately disposed of by reusing it as renewable energy [70]. As the ratio of blending for bio-waste increased, the HHVs increased more than the FS; the energy density of the subsequent bio-solid also increased. Sewage sludge and *Leucaena* co-torrefaction produced a similar outcome. When bio-solid was created from torrefied food scraps, it had a significantly higher HHV than bio-solid created from torrefied food scraps alone (19.2–20 MJ/kg). The HHV content of FS with MH (25/75% dry basis) presented the highest amount of investigational HHV [41].

This is consistent with those previously described for torrefied wood and agricultural biomass after hydrothermal carbonization. The higher degree of carbonization of torrefaction significantly accelerated cellulose and hemicellulose degradation, resulting in a reduction in smoke (from fly ash, CO_x, NO_x, and SO_x) produced during bio-fuel combustion [71]. The increase in the temperature and reaction time of torrefaction steadily increases the HHV. The result is affected more by the reactor time of co-torrefaction than by the temperature of the OS bio-solid. The heating value of the bio-solid was 24.1 MJ/kg, at a temperature of 300 °C at a residence time of 45 min. The blended FS bio-solid had a maximum heating value of 18.9 MJ/kg at 150 °C at 30 min. The HHV of bio-solid from FS was 21.7% higher than that of the raw sludge [41]. The increase in torrefaction temperature decreased the mass yield from 84.2% (120 °C for 30 min) to 67.7% (200 °C for 30 min). It could be associated with protein breakdown and polysaccharides in solids of sludge [72].

3.3.3. Van Krevelen Diagram

The Van Krevelen diagram was first used to categorize the coal and estimate the compositional change throughout maturity by plotting O/C against H/C. In order to better understand fuel quality, one must consider the atomic ratios of the constituting elements. The HHV of biomass, for example, ranged from approximately 20.5 to 15 MJ/kg as the oxygen–carbon ratio increased from 0.86 to 1.03 [73].

The Van Krevelen diagram also compares torrefied and untorrefied biomass. Torrefied biomass has a higher carbon content and decreases oxygen and hydrogen contents compared to untorrefied biomass. The other aspect is that co-torrefied biomass has lower oxygen-to-carbon and hydrogen-to-carbon ratios compared to untorrefied biomass, as presented in Figure 4. Untorrefied biomass, such as OS 100%, MIse 100%, EFB 100%, Cv 100%, and Lc 100%, have low HHVs due to the higher O/C and H/C ratios, and co-torrefied biomass, such as OS:MIse (25:75%) torrefied = 150 °C, EFB with used UCO torrefied = 300 °C, Lc 50% torrefied = 300 °C, and Lc 100% torrefied = 300 °C, have high HHVs due to the low O/C ratio, as depicted in Figure 4. This discussion shows that torrefied biomass has better fuel than untorrefied biomass.

Figure 4 also presents the O/C and H/C values of the coal. Anthracite has elaborated low values of the O/C and H/C ratios and presents high-solid-fuel properties. After comparing the torrefied with untorrefied biomass in different literature surveys, it can be observed that the un-torrefied biomass outlies the coal value of the O/C and H/C ratios. However, the ratios of H/C and O/C of the torrefied biomass are close to those for coal. For example, EFB pellets with UCO, T = 300 °C show that the O/C- and H/C-ratio values are very similar to anthracite coal, showing that this biomass has a good fuel quality.

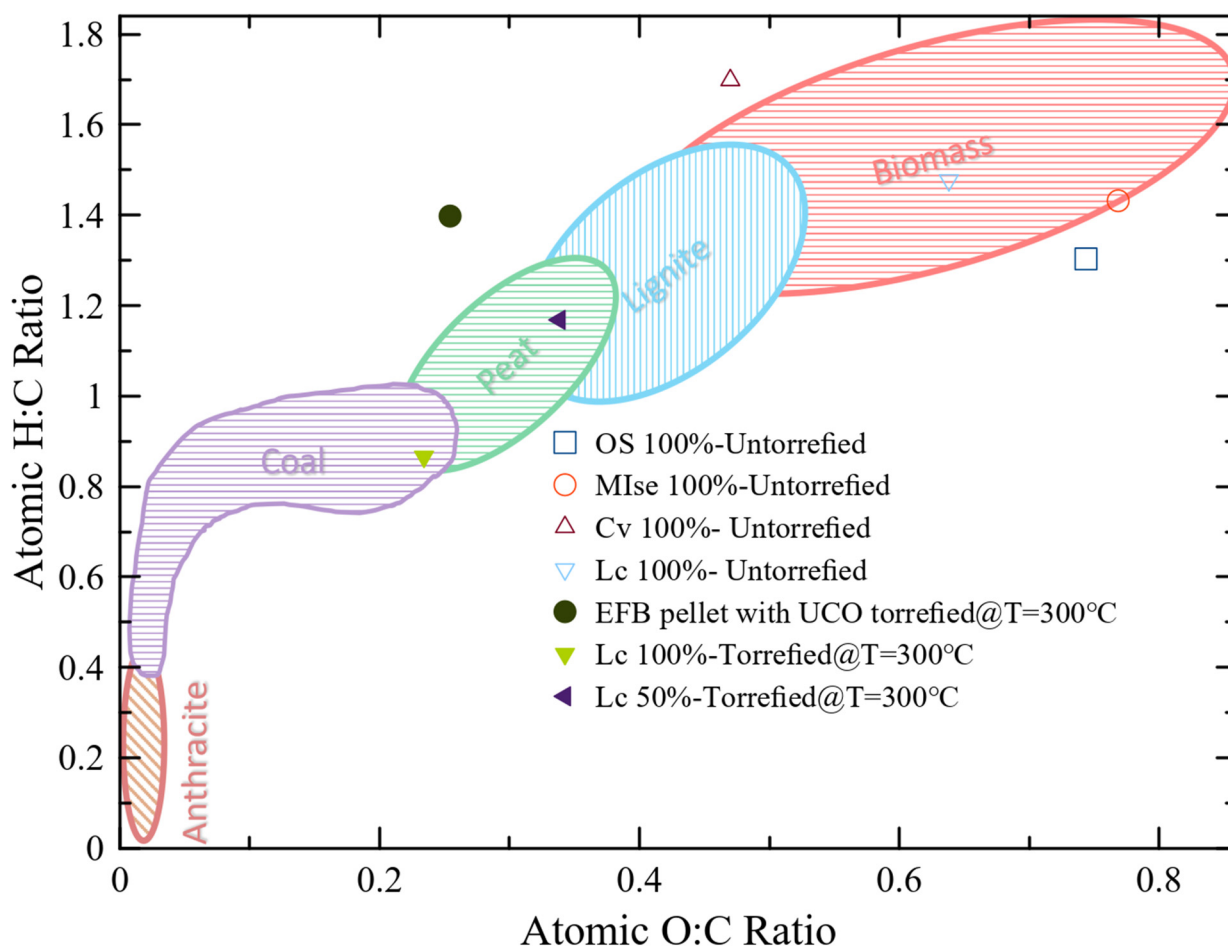


Figure 4. Van Krevelen diagram redrawn using the data from [74].

Fuel quality decreases as the O/C and H/C ratios increase. A decrease in the O/C ratio was compared to the raw materials Cv and Lc in bio-solids formed at 200 °C and 225 °C, indicating some deoxygenation. However, no structural alterations were observed because the H/C ratio was equivalent to the feedstock. Thermal processes, such as bio-solid torrefaction, results in O/C and H/C ratios compared to peat, lignite, and anthracite coal, further demonstrating the impact of temperature on fuel quality [29]. A temperature-dependent decrease in the H/C ratio was also observed at co-torrefaction temperatures higher than 250 °C. This indicates that the carbonaceous structure is reorganized as more aromatic compounds are produced [75]. The lignocellulosic structure of the bio-solid undergoes an enhanced rearrangement under high-torrefaction conditions, altering the porosity of the material by eliminating OH-binding groups [76]. Compared to raw biomasses, bio-solids also have a higher energy content due to their lower moisture content [74]. The calorific value of co-torrefied biomasses depends on the oxygen, hydrogen, and carbon content present in the feed. The feed contains a significant amount of oxygen and a low carbon content, so its calorific value is low and vice versa [77]. The primary objective of pre-treatment is to improve the carbon content and reduce the oxygen level. Co-torrefaction is used to reduce the oxygen concentration of biomass, which directly affects the heating value of any fuel and presents a higher calorific value. As a result, it is challenging to convert biomass into liquid fuels with an improved heating value. Products can be produced from the biomass of high-oxygen or -hydrogen contents [56].

4. Reactor for Co-Torrefaction Technology

Numerous reactor configurations are reported for use in the co-torrefaction process and are explained below.

4.1. Conventional/Fixed-Bed Reactor

The experiments conducted on a smaller scale, such as those conducted in a laboratory, frequently use a fixed-bed reactor. Before being placed into the reactor, biomass is typically dried and co-torrefied in a furnace [78]. According to the authors, this was the most straightforward reactor configuration for biomass co-torrefaction [78]. At the end of the process, the biomass was cooled and collected for further study. Temperatures were evenly distributed throughout the sample due to the biomass being covered in a crucible. Additionally, the biomass was placed for a specific time, and a heating rate was chosen for use in biomass blends. At a certain flow rate of gas, nitrogen gas (N₂) was supplied to displace the air. The gas entered the reactor by the gas inflow located at the top, and it left the reactors from the bottom [79].

4.2. Fluidizing-Bed Reactor

The co-torrefaction process was also performed in the fluidized-bed reactor (Figure 5), where the biomass particles interact with the gas stream. In the co-torrefaction process, a multicomponent bed is selected for biomass particles. For example, biomass and coal sludge particles use a multicomponent, such as coal sludge and a straw pellet bed. The fractional content of the coal sludge varied according to the particle size distribution. The “cold” model was tested using an acrylic glass column that allowed a visual examination and a piece of equipment to have some length, width, and height. The column was supported by a perforated plate that served as an air-distribution grille. A net was attached to the grill top to prevent the mixture from clogging up the holes. The air-distribution grille of the device was supported by an air-suction chamber equipped with Raschig rings beneath the fluidized bed, which helped smooth the airflow. A blower with a pressure head was used to introduce ambient air into the fluidized bed [80]. The flow rate was measured, and airflow control was performed using a bypass conduit that bypassed airflow through a hose. The air velocity leaving the device was determined using a hot wire anemometer. Each experiment consisted of observations of air velocity. The transition from mono-disperse to fluidized state occurred in a poly-disperse particle bed, particularly when the particles

had a variety of shapes and sizes [81,82]. The minimal fluidization velocity of a mixture of particles was hypothesized to be defined by a linear connection between the variance of the pressure difference between them and its mean value, and thus the velocity of the gas blown over the bed [80,83].

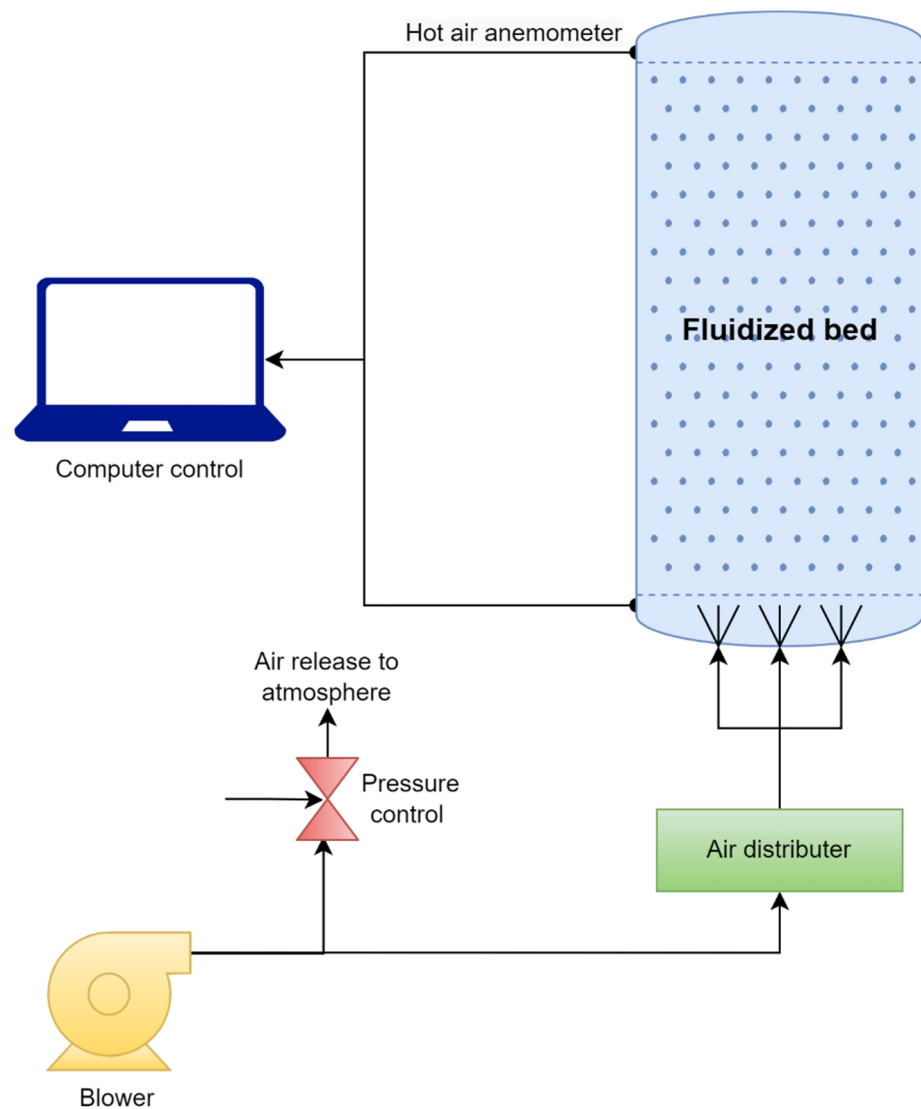


Figure 5. Fluidized-bed reactor adapted adapted from [84].

4.3. Microwave Reactor

This reactor type is discussed using the example of various biomasses. This experiment utilized a co-torrefied reactor and a microwave heating reactor. The exact ratio of feedstock combination was used three times without using a microwave absorbent in the microwave co-torrefaction (MCT) process. Through dipolar polarization, ionic conduction, and interface polarization, microwave irradiation caused the particles to become internally heated. In recent years, a progressive shift away from traditional torrefaction and towards more productive microwave torrefaction has been observed [85]. As shown in Figure 6, microwave power is used to conduct the process [30]; the physical and chemical characteristics of the bio-solid formed result from the torrefaction of biomass in a microwave reactor. Significant process factors that affect the quality of the bio-solid produced by microwave reactor torrefaction include the microwave cavity mode, microwave power, temperature, reaction time, and biomass moisture content. Meanwhile, the modification of the mixer and the addition of multiple magnetron units are recommended to overcome the

uneven distribution of microwave heating. The quality of the bio-solid is also influenced by the kind of biomass used, as various feedstocks have different optimum torrefaction conditions [86].

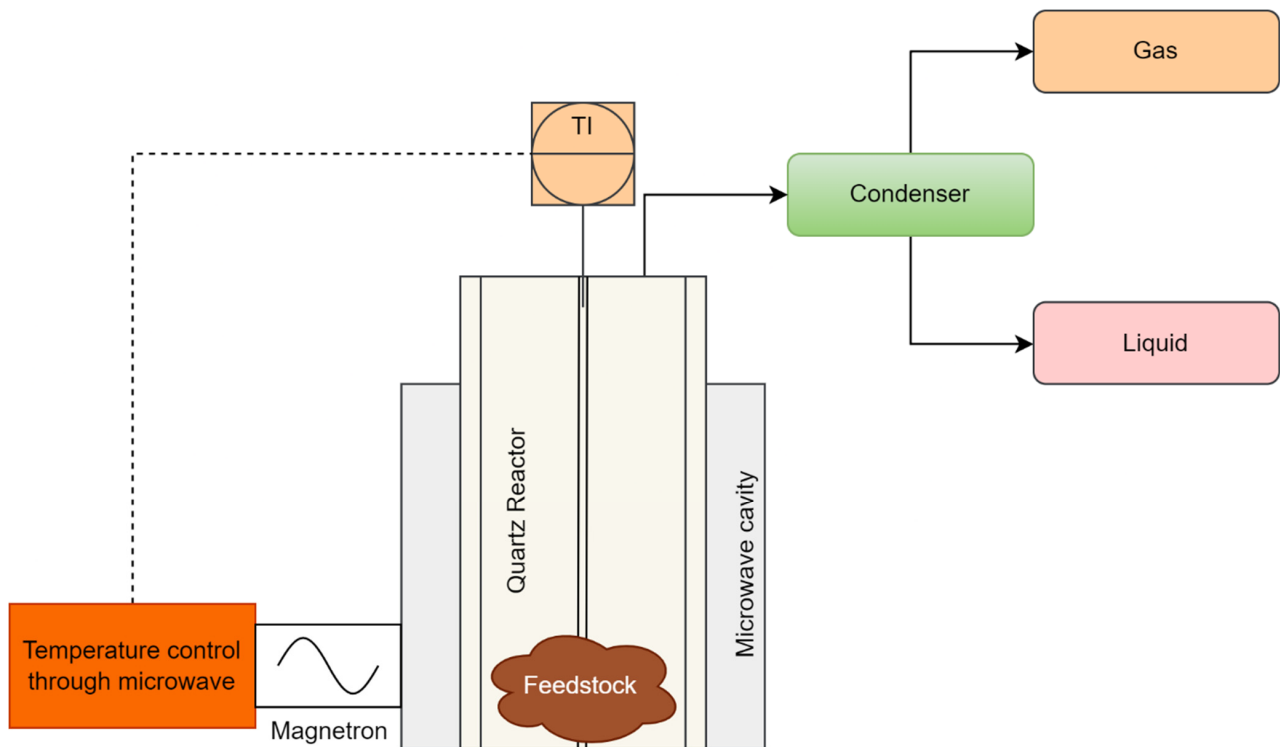


Figure 6. Microwave heat reactor adapted from [30].

4.4. Co-Torrefaction in a Batch Reactor

The co-torrefaction technique is used to produce bio-char in batch reactors. Figure 7 is a schematic diagram of a batch-type reactor system. The entire system can be divided into three sections: the entrance, the main body, and the output. The intake section consists of a nitrogen gas cylinder and a flow meter. The nitrogen flow rate was set at a specific value. The primary component of this system was a glass tube. The study was conducted to improve the synergistic effect of bio-solids [87]. The research was conducted to determine whether co-torrefaction with intermediate waste has a synergistic impact, using a different type of biomass in a batch reactor to improve the bio-solid. The interaction was evaluated using the synergistic effect ratio [87].

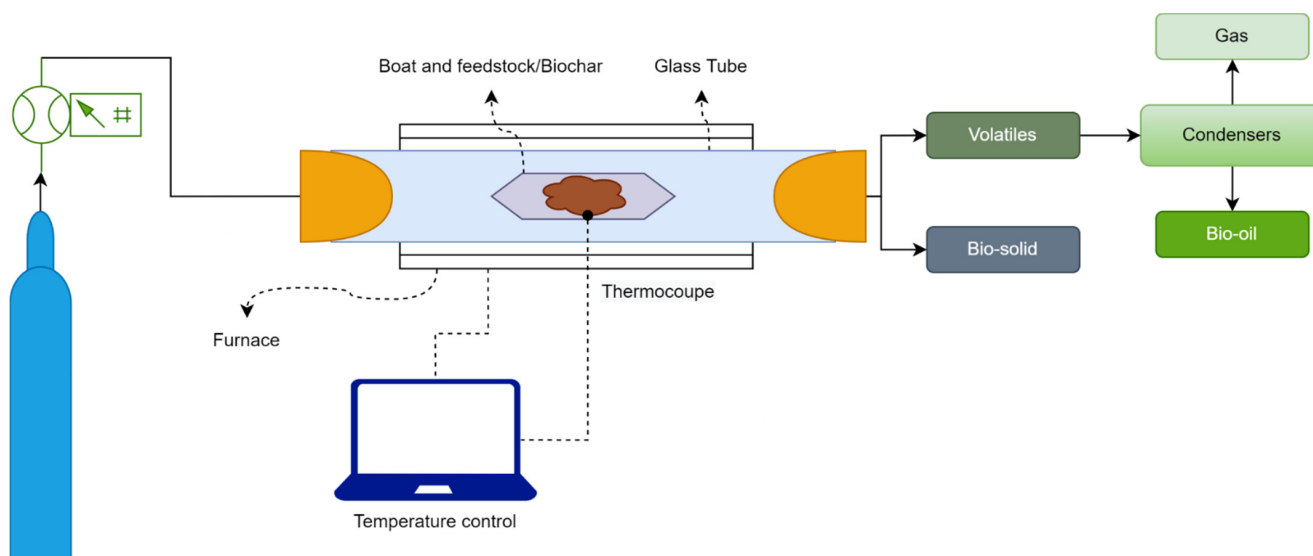


Figure 7. Setup of bio-char production through the co-torrefaction process adapted from [87].

A boat, hook, and furnace equipped with a thermocouple helped to control the furnace temperature. The co-torrefaction ingredients were loaded into the boat. Materials weighing around 30 grams were used for each run. Two plugs were used to secure the boat and seal the glass tube. A hook was inserted into the plug to monitor the whereabouts of the boat. In the furnace, a glass tube with a boat and a thermocouple attached to the center of the sample pile was inserted and heated [88]. The accessory was used to draw the co-torrefied biomass boat (char) out of the glass tube when the co-torrefaction phase was completed. The weight percent of the char to the raw biomass was used to calculate the solid output. Two cylinders and a cooling system were added to the output section of the system. A water-coated glass tube was used to cool the device. After the thermal decomposition process was completed, the unit was cooled down and shut down. The primary consideration was maintaining a constant temperature throughout the batch reactor as the torrefaction process occurred. This was performed, and the bio-solid product was completely under control [89].

5. Application of the Co-Torrefaction Process

Co-torrefaction is used for various applications, including improving bio-char and CO₂ adsorption.

5.1. Biochar Enhancement

Although tar was previously believed to be the primary energy source in the liquid product, numerous experimental experiments have been published in the literature [90,91]. It was treated as an undesirable result of torrefaction. Tar was choking the facilities or pipes [92]. Its high viscosity was related to the existence of several heavy chemicals. Oil, on the other hand, lacked significant HHV concentration. However, its lower viscosity made it easier for real-world applications [93,94]. Tar, on the other hand, has a much higher HHV concentration than oil. Bio-char was coated with a new method of reusing tar following the principles of sustainability and the circular economy, which improved its HHV. Tar was pipetted into charcoal at a volume of 0.5 mL, followed by at least 12 h of roasting to verify that the enhanced bio-char had the same dry foundation as the raw bio-char for the HHV measurement. Pre- and post-modification increased the HHV.

Furthermore, the HHV of the tar was improved with a ratio of Fir 60 to WE2 60 to Fir 40 to WE1 60 to Fir 20 [87]. The coating procedure must be constant across all samples to ensure that the two orders are similar. The increase in bio-char porosity helped the tar adsorption of raw biomass [95]. The waste-to-energy approach, which used recycled tar

to increase the HHV content of bio-char, was an effective way to remove an unwanted by-product and treat it as a useful component [96].

5.2. CO₂ Adsorption through Bio-Solid via the Co-Torrefaction Method

Bio-solids for CO₂ adsorption were prepared using sewage sludge and Leucaena wood by microwave co-torrefaction. Sludge-to-wood ratios of 75:25, 50:50, and 25:75% were used to produce a bio-solid as the adsorption of CO₂ [44]. The carbon and fixed carbon content of Leucaena wood increased, even if the mass and energy yields of the wood decreased. Carbon-rich bio-solid can absorb more CO₂ molecules than a lower carbon-rich bio-solid [97]. The adsorption capacity is about four times greater for the pure Leucaena bio-solid than for the pure sewage bio-solid. Increasing the amount of Leucaena wood in the mixture would have a negative impact on the composition or characteristics of the bio-solid, resulting in the adsorption of CO₂ in the bio-solid. When it comes to the adsorption of CO₂ on the bio-solid surface, the adsorption reaction can control how well the intra-particle diffusion kinetic model performs [44].

The adsorption of CO₂ increased with a higher concentration of the Leucaena wood mixture. The pure Leucaena bio-solid had an adsorption capacity of approximately four times that of the pure-sewage bio-solid. According to the results, the observed CO₂ adsorption capacity was close to the predicted values of 0.75 or 0.50. Unfortunately, the measured adsorption capacity was less than predicted for a mixing ratio of 0.25 [98]. Thus, the experimental outcome was lower than that predicted in theory. The significant usage of Leucaena wood in bio-solids can have a detrimental effect on its composition or properties, resulting in a lower capacity to absorb CO₂. To fully understand this occurrence, more research is necessary. The carbon-rich bio-solid could absorb more CO₂ molecules than bio-solids with a lower carbon content. Pure bio-char manufactured from Leucaena wood has four times the absorption capacity of pure bio-solid generated from pine wood [68].

5.3. Renewable Fuel for Gasification

Torrefaction is mainly used as a pre-treatment process to improve sustainable and renewable biofuels. This biofuel may be used in alternative bioenergy-production processes. Torrefied biomass (wood) is primarily used as biofuel production for gasification [99]. The experimental study supports the stated advantages of gasification combined with torrefaction. The experiments involved the gasification of torrefied beech wood in an entrained flow (EF) reactor. Torrefaction has been shown to decrease the O/C ratio in biomass and improve the quality of syngas. Torrefied wood gasification yields 6.5% more hydrogen, 20% more carbon monoxide, and approximately the same level of carbon dioxide as original wood [100]. Combining the torrefaction of agricultural waste well with the co-gasification of coal in an entrained flow gasifier [101] improved the fuel quality. The advantages of this method include the fact that the torrefaction facility can be close to the gasifier (the mill can grind both torrefied biomass and coal), torrefaction gas can be used as an energy source in the pyrolysis reactor, the torrefaction liquids can be mixed with a coal slurry, and the gasification of the wet biomass is enhanced [102].

6. Circular Economy

Understanding the waste economy has promoted valuation strategies to reduce resource wastage [103]. Rapid industrialization, increased human population, ongoing environmental impacts, and energy security have contributed to a widespread acceptance of the need to change from a linear to circular economy (CE) [104]. The idea of the CE is closely related to the philosophy of environmentally friendly practices. It offers an alternative framework that emphasizes a significant decrease in adverse effects on the environment and the development of new commercial prospects [105]. The linear economic model based on the overall approach of “extract, use, and dispose of operations” is generally unsustainable, leading to many environmental concerns and challenges with respect to energy security. Torrefaction is mainly used as a pre-treatment process to improve sustainable and

renewable biofuels. This biofuel may be used in alternative bioenergy-production processes. Torrefied biomass (wood) is primarily used as a biofuel-production process for gasification.

Moreover, this model has been the primary cause of these problems. The CE framework encourages industrialization operations to study ways in which they might make more effective use of their resources and outputs. This is one of the objectives of the CE framework [103]. This involves the optimal use of waste products, such as the thermochemical conversion process (co-torrefaction) of bio-waste. The considerable increase in population and urbanization led to an instant increase in the waste produced [106]. The technology and methods required to manage and treat waste are, at present, in existence and have reached a mature stage, particularly in developed countries. Despite this, it is still predicted that trash will continue to be a burden on the environment and a contributor to the spread of the CE. Therefore, it offers prosperity for employment to manufacture goods with value additions and energy. The waste classified as biomass originates from living biological entities, such as plants and animals.

In addition, waste products and residues derived from agriculture and neighboring industries are included. For the longest period of time, waste from these sources has been frequently used as a low-cost energy source. This includes the use of solid fuels, such as pellets and briquettes, and more advanced bioenergy products [107]. However, the more economical use of these wastes considerably depends on the suitable expansion of available bio-compounds other than bioenergy. This is because bioenergy is a somewhat limited resource. This is one of the significant aspects that must be developed to create technologies that can generate a variety of organic goods that are commercially viable. The co-torrefaction of various waste streams, such as sewage sludge and bio-wastes, is a reasonable solution that can help develop waste-mitigation techniques, as stated by several industry experts [23]. The improved fuel characteristics of the bio-solid that was generated were achieved by applying microwave co-torrefaction of an EFB [30]. Using MCT, the researchers discovered that they could produce torrefied biomass with a heating value of 28 MJ/kg, a mass yield of 85.5%, and a fuel-to-energy ratio of 1.8, all of which contributed to the CE [30].

7. Research Gaps and Recommendations

Co-torrefaction-related factors and how they affect various other processing stages were studied. Future research goals might consist of the following:

- Co-torrefaction techniques depend on the activation energies to degrade cellulose, hemicelluloses, and lignin.
- Co-torrefaction may be examined at the microscopic level by identifying unique functional groups and determining the energy required to cleave bonding bonds.
- Utilizing Fourier transform infrared (FTIR) and Raman spectroscopy to study the spontaneous co-torrefaction process.
- Using the Hunter colorimeter, determine the level of co-torrefaction severity predicated on color changes.
- Thermogravimetric analysis was utilized to investigate the kinetics of weight reduction.
- Investigating how various temperatures affect the structure of biomass.
- Integration of co-torrefaction and densification as part of an integrated operation.
- Method to calculate the energy required for the production of condensable and non-condensable products through co-torrefaction.
- The off-gassing and spontaneous combustion behaviors of co-torrefied biomass stored at various storage temperatures are suggested.
- The recommendation process of the co-torrefaction process.
- It is essential to comprehend the environmental aspects of alternative fuel techniques if one is interested in generating environmentally friendly fuels.
- It is possible to significantly reduce emissions by increasing the properties of biomass fuels. Consequently, biomass must be processed before being used in energy applications to optimize its fuel properties. Considering the environmental impact of

pre-treatment procedures is essential because they use large amounts of energy and other resources.

- Life cycle analysis (LCA) is the most widely used method for determining whether a bioenergy system is environmentally feasible.
- Thus, a key component in controlling the release of prospective greenhouse gas emissions throughout the co-torrefaction process is the thermal energy source employed in drying through the co-torrefaction process. Therefore, such emissions can be reduced by adopting renewable fuels as a heat source.

8. Conclusions

The potential of biomass blends of various intermediate bio-wastes' pre-treatment through the co-torrefaction process made using co-torrefied biomass is a good competitor for energy generation. The bio-solid was deoxygenated, decarboxylated, and dehydrated for the final compositions during the co-torrefied samples. HHV, fixed carbon content, and energy density were found in bio-solids generated from feedstock that were only co-torrefied or in respect of different mixing ratios. As a result, co-torrefaction provides an option for converting bio-waste into biofuels with high efficiency. Additional studies may be conducted to economically evaluate and fully demonstrate the possibility of co-torrefaction for using bio-waste in actual applications, such as being utilized as industrial furnaces and boiler fuels. The standard for sub-bituminous and anthracite coal with low ash and sulfur contents is to reduce GHG emissions. Consequently, it is considered a potentially useful method for manufacturing high-quality products and biofuels that can serve as an alternative to bio-waste disposal while reducing the concerns.

Author Contributions: Conceptualization, S.R.N.; methodology, S.R.N., A.W. and I.A.; software, I.A.; validation, A.W., S.R.N. and I.A.; formal analysis, I.A.; investigation, A.W. and I.A.; resources, S.R.N.; data curation, A.W.; writing—original draft preparation, A.W. and I.A.; writing—review and editing, S.R.N. and I.A.; visualization, I.A.; supervision, S.R.N.; project administration, S.R.N. All authors have read and agreed to the published version of the manuscript.

Funding: This research received no external funding.

Data Availability Statement: Not applicable.

Conflicts of Interest: The authors declare no conflict of interest.

References

1. Wang, T.; Zhai, Y.; Li, H.; Zhu, Y.; Li, S.; Peng, C.; Wang, B.; Wang, Z.; Xi, Y.; Wang, S.; et al. Co-hydrothermal carbonization of food waste-woody biomass blend towards biofuel pellets production. *Bioresour. Technol.* **2018**, *267*, 371–377. [[CrossRef](#)] [[PubMed](#)]
2. Zhu, Z.; Si, B.; Lu, J.; Watson, J.; Zhang, Y.; Liu, Z. Elemental migration and characterization of products during hydrothermal liquefaction of cornstalk. *Bioresour. Technol.* **2017**, *243*, 9–16. [[CrossRef](#)] [[PubMed](#)]
3. Abdalla, M.E.; Abdalla, S.A.; Taqvi, S.A.; Naqvi, S.R.; Chen, W.-H. Investigation of Biomass Integrated Air Gasification Regenerative Gas Turbine Power Plants. *Energies* **2022**, *15*, 741. [[CrossRef](#)]
4. Ge, S.; Foong, S.Y.; Ma, N.L.; Liew, R.K.; Mahari, W.A.W.; Xia, C.; Yek, P.N.Y.; Peng, W.; Nam, W.L.; Lim, X.Y.; et al. Vacuum pyrolysis incorporating microwave heating and base mixture modification: An integrated approach to transform biowaste into eco-friendly bioenergy products. *Renew. Sustain. Energy Rev.* **2020**, *127*, 109871. [[CrossRef](#)]
5. Naqvi, S.R.; Taqvi, S.A.A.; Mehran, M.T.; Khoja, A.H.; Naqvi, M.; Bokhari, A.; Saidina Amin, N.A. Chapter 2-Catalytic pyrolysis of biomass using shape-selective zeolites for bio-oil enhancement. In *Bioenergy Resources and Technologies*; Azad, A.K., Khan, M.M.K., Eds.; Academic Press: Cambridge, MA, USA, 2021; pp. 39–60.
6. Zafar, M.W.; Shahbaz, M.; Hou, F.; Sinha, A. From nonrenewable to renewable energy and its impact on economic growth: The role of research & development expenditures in Asia-Pacific Economic Cooperation countries. *J. Clean. Prod.* **2019**, *212*, 1166–1178.
7. Qayyum, M.; Khoja, A.H.; Naqvi, S.R.; Ejaz, H.; Nawar, A.; Ansari, A.A. Development of Cost-Effective Fertilizer-Based Media for the Microalgae Cultivation Aimed at Effective Biomass Production. *NUST J. Eng. Sci.* **2020**, *13*, 45–51.
8. Antar, M.; Lyu, D.; Nazari, M.; Shah, A.; Zhou, X.; Smith, D.L. Biomass for a sustainable bioeconomy: An overview of world biomass production and utilization. *Renew. Sustain. Energy Rev.* **2021**, *139*, 110691. [[CrossRef](#)]
9. Chen, W.-H.; Farooq, W.; Shahbaz, M.; Naqvi, S.R.; Ali, I.; Al-Ansari, T.; Saidina Amin, N.A. Current status of biohydrogen production from lignocellulosic biomass, technical challenges and commercial potential through pyrolysis process. *Energy* **2021**, *226*, 120433. [[CrossRef](#)]

10. Khan, M.; Raza Naqvi, S.; Ullah, Z.; Ali Ammar Taqvi, S.; Nouman Aslam Khan, M.; Farooq, W.; Taqi Mehran, M.; Juchelková, D.; Štěpanec, L. Applications of machine learning in thermochemical conversion of biomass—A review. *Fuel* **2023**, *332*, 126055. [[CrossRef](#)]
11. Ellabban, O.; Abu-Rub, H.; Blaabjerg, F. Renewable energy resources: Current status, future prospects and their enabling technology. *Renew. Sustain. Energy Rev.* **2014**, *39*, 748–764. [[CrossRef](#)]
12. Cheng, Y.W.; Chong, C.C.; Lee, S.P.; Lim, J.W.; Wu, T.Y.; Cheng, C.K. Syngas from palm oil mill effluent (POME) steam reforming over lanthanum cobaltite: Effects of net-basicity. *Renew. Energy* **2020**, *148*, 349–362. [[CrossRef](#)]
13. Farooq, W.; Ali, I.; Raza Naqvi, S.; Sajid, M.; Abbas Khan, H.; Adamu, S. Evolved Gas Analysis and Kinetics of Catalytic and Non-Catalytic Pyrolysis of Microalgae *Chlorella* sp. Biomass With Ni/ θ -Al₂O₃ Catalyst via Thermogravimetric Analysis. *Front. Energy Res.* **2021**, *9*, 775037. [[CrossRef](#)]
14. Moriarty, P.; Honnery, D. Global Renew. Energy resources and use in 2050. In *Managing Global Warming*; Elsevier: Amsterdam, The Netherlands, 2019; pp. 221–235.
15. Raza, M.; Inayat, A.; Ahmed, A.; Jamil, F.; Ghenai, C.; Naqvi, S.R.; Shanableh, A.; Ayoub, M.; Waris, A.; Park, Y.-K. Progress of the Pyrolyzer Reactors and Advanced Technologies for Biomass Pyrolysis Processing. *Sustainability* **2021**, *13*, 11061. [[CrossRef](#)]
16. Wen, J.-L.; Sun, S.-L.; Yuan, T.-Q.; Xu, F.; Sun, R.-C. Understanding the chemical and structural transformations of lignin macromolecule during torrefaction. *Appl. Energy* **2014**, *121*, 1–9. [[CrossRef](#)]
17. Mamvura, T.A.; Danha, G. Biomass torrefaction as an emerging technology to aid in energy production. *Heliyon* **2020**, *6*, e03531. [[CrossRef](#)]
18. Mahari, W.A.W.; Chong, C.T.; Lam, W.H.; Anuar, T.N.S.T.; Ma, N.L.; Ibrahim, M.D.; Lam, S.S. Microwave co-pyrolysis of waste polyolefins and waste cooking oil: Influence of N₂ atmosphere versus vacuum environment. *Energy Convers. Manag.* **2018**, *171*, 1292–1301. [[CrossRef](#)]
19. Lam, S.S.; Mahari, W.A.W.; Jusoh, A.; Chong, C.T.; Lee, C.L.; Chase, H.A. Pyrolysis using microwave absorbents as reaction bed: An improved approach to transform used frying oil into biofuel product with desirable properties. *J. Clean. Prod.* **2017**, *147*, 263–272. [[CrossRef](#)]
20. Uemura, Y.; Sellappah, V.; Trinh, T.H.; Hassan, S.; Tanoue, K.-I. Torrefaction of empty fruit bunches under biomass combustion gas atmosphere. *Bioresour. Technol.* **2017**, *243*, 107–117. [[CrossRef](#)]
21. Atabani, A.E.; Pugazhendhi, A.; Almomani, F.; Rene, E.R.; Naqvi, S.R. Recent advances in the thermochemical transformation of biomass to bio-oil, biochar and syngas and its upgrading methods. *Process Saf. Environ. Prot.* **2022**, *168*, 624–625. [[CrossRef](#)]
22. Khan, A.A.; Gul, J.; Naqvi, S.R.; Ali, I.; Farooq, W.; Liaqat, R.; AlMohamadi, H.; Štěpanec, L.; Juchelková, D. Recent progress in microalgae-derived biochar for the treatment of textile industry wastewater. *Chemosphere* **2022**, *306*, 135565. [[CrossRef](#)]
23. Zheng, N.-Y.; Lee, M.; Lin, Y.-L. Co-processing textile sludge and lignocellulose biowaste for biofuel production through microwave-assisted wet torrefaction. *J. Clean. Prod.* **2020**, *268*, 122200. [[CrossRef](#)]
24. Inayat, M.; Shahbaz, M.; Naqvi, S.R.; Sulaiman, S.A. Chapter 3—Advance strategies for tar elimination from biomass gasification techniques. In *Bioenergy Resources and Technologies*; Azad, A.K., Khan, M.M.K., Eds.; Academic Press: Cambridge, MA, USA, 2021; pp. 61–88.
25. Sajdak, M. Impact of plastic blends on the product yield from co-pyrolysis of lignin-rich materials. *J. Anal. Appl. Pyrolysis* **2017**, *124*, 415–425. [[CrossRef](#)]
26. Wu, W.; Qiu, K. Vacuum co-pyrolysis of Chinese fir sawdust and waste printed circuit boards. Part I: Influence of mass ratio of reactants. *J. Anal. Appl. Pyrolysis* **2014**, *105*, 252–261. [[CrossRef](#)]
27. Wang, L.; Barta-Rajnai, E.; Skreiberg, Ø.; Khalil, R.; Czégény, Z.; Jakab, E.; Barta, Z.; Grønli, M. Effect of torrefaction on physicochemical characteristics and grindability of stem wood, stump and bark. *Appl. Energy* **2018**, *227*, 137–148. [[CrossRef](#)]
28. Yek, P.N.Y.; Mahari, W.A.W.; Kong, S.H.; Foong, S.Y.; Peng, W.; Ting, H.; Liew, R.K.; Xia, C.; Sonne, C.; Tabatabaei, M.; et al. Pilot-scale co-processing of lignocellulosic biomass, algae, shellfish waste via thermochemical approach: Recent progress and future directions. *Bioresour. Technol.* **2022**, *347*, 126687. [[CrossRef](#)]
29. Chen, W.-H.; Lin, B.-J.; Lin, Y.-Y.; Chu, Y.-S.; Ubando, A.T.; Show, P.L.; Ong, H.C.; Chang, J.-S.; Ho, S.-H.; Culaba, A.B.; et al. Progress in biomass torrefaction: Principles, applications and challenges. *Prog. Energy Combust. Sci.* **2021**, *82*, 100887. [[CrossRef](#)]
30. Lam, S.S.; Tsang, Y.F.; Yek, P.N.Y.; Liew, R.K.; Osman, M.S.; Peng, W.; Lee, W.H.; Park, Y.-K. Co-processing of oil palm waste and waste oil via microwave co-torrefaction: A waste reduction approach for producing solid fuel product with improved properties. *Process Saf. Environ. Prot.* **2019**, *128*, 30–35. [[CrossRef](#)]
31. Gadd, G.M. Biosorption: Critical review of scientific rationale, environmental importance and significance for pollution treatment. *J. Chem. Technol. Biotechnol. Int. Res. Process Environ. Clean Technol.* **2009**, *84*, 13–28. [[CrossRef](#)]
32. Mehdi, R.; Khoja, A.H.; Naqvi, S.R.; Gao, N.; Amin, N.A. A Review on Production and Surface Modifications of Biochar Materials via Biomass Pyrolysis Process for Supercapacitor Applications. *Catalysts* **2022**, *12*, 798. [[CrossRef](#)]
33. Khan, S.A.; Ali, I.; Naqvi, S.R.; Li, K.; Mehran, M.T.; Khoja, A.H.; Alarabi, A.A.; Atabani, A.E. Investigation of slow pyrolysis mechanism and kinetic modeling of *Scenedesmus quadricauda* biomass. *J. Anal. Appl. Pyrolysis* **2021**, *158*, 105149. [[CrossRef](#)]
34. Madhu, P.; Vidhya, L.; Vinodha, S.; Wilson, S.; Sekar, S.; Patil, P.P.; Kaliappan, S.; Prabhakar, S. Co-pyrolysis of Hardwood Combined with Industrial Pressed Oil Cake and Agricultural Residues for Enhanced Bio-Oil Production. *J. Chem.* **2022**, *2022*, 9884766. [[CrossRef](#)]

35. Viegas, C.; Nobre, C.; Correia, R.; Gouveia, L.; Gonçalves, M. Optimization of Biochar Production by Co-Torrefaction of Microalgae and Lignocellulosic Biomass Using Response Surface Methodology. *Energies* **2021**, *14*, 7330. [[CrossRef](#)]
36. Cahyanti, M.N.; Doddapaneni, T.R.K.C.; Kikas, T. Biomass torrefaction: An overview on process parameters, economic and environmental aspects and recent advancements. *Bioresour. Technol.* **2020**, *301*, 122737. [[CrossRef](#)]
37. Sharma, H.B.; Dubey, B.K. Binderless fuel pellets from hydrothermal carbonization of municipal yard waste: Effect of severity factor on the hydrochar pellets properties. *J. Clean. Prod.* **2020**, *277*, 124295. [[CrossRef](#)]
38. Chen, W.-H.; Kuo, P.-C. A study on torrefaction of various biomass materials and its impact on lignocellulosic structure simulated by a thermogravimetry. *Energy* **2010**, *35*, 2580–2586. [[CrossRef](#)]
39. Yan, W.; Acharjee, T.C.; Coronella, C.J.; Vasquez, V.R. Thermal pretreatment of lignocellulosic biomass. *Environ. Prog. Sustain. Energy* **2009**, *28*, 435–440. [[CrossRef](#)]
40. Kethobile, E.; Ketlogetswe, C.; Gandure, J. Torrefaction of non-oil *Jatropha curcas* L. (*Jatropha*) biomass for solid fuel. *Heliyon* **2020**, *6*, e05657. [[CrossRef](#)]
41. Zheng, N.-Y.; Lee, M.; Lin, Y.-L.; Samannan, B. Microwave-assisted wet co-torrefaction of food sludge and lignocellulose biowaste for biochar production and nutrient recovery. *Process Saf. Environ. Prot.* **2020**, *144*, 273–283. [[CrossRef](#)]
42. Yek, P.N.Y.; Chen, X.; Peng, W.; Liew, R.K.; Cheng, C.K.; Sonne, C.; Sii, H.S.; Lam, S.S. Microwave co-torrefaction of waste oil and biomass pellets for simultaneous recovery of waste and co-firing fuel. *Renew. Sustain. Energy Rev.* **2021**, *152*, 111699. [[CrossRef](#)]
43. Li, J.; Brzdekiewicz, A.; Yang, W.; Blasiak, W. Co-firing based on biomass torrefaction in a pulverized coal boiler with aim of 100% fuel switching. *Appl. Energy* **2012**, *99*, 344–354. [[CrossRef](#)]
44. Huang, Y.-F.; Chiueh, P.-T.; Lo, S.-L. CO₂ adsorption on biochar from co-torrefaction of sewage sludge and leucaena wood using microwave heating. *Energy Procedia* **2019**, *158*, 4435–4440. [[CrossRef](#)]
45. Rizkiana, J.; Zahra, A.; Wulandari, W.; Saputra, W.; Andrayukti, R.; Sianipar, A.; Sasongko, D. Effects of Coal and Biomass Types towards the Quality of Hybrid Coal Produced via Co-Torrefaction. *IOP Conf. Ser. Mater. Sci. Eng.* **2020**, *823*, 012028. [[CrossRef](#)]
46. Lin, Y.-L.; Zheng, N.-Y. Biowaste-to-biochar through microwave-assisted wet co-torrefaction of blending mango seed and passion shell with optoelectronic sludge. *Energy* **2021**, *225*, 120213. [[CrossRef](#)]
47. Liu, X.; Lin, Q.; Yan, Y.; Peng, F.; Sun, R.; Ren, J. Hemicellulose from plant biomass in medical and pharmaceutical application: A critical review. *Curr. Med. Chem.* **2019**, *26*, 2430–2455. [[CrossRef](#)] [[PubMed](#)]
48. Rago, Y.P.; Collard, F.-X.; Görgens, J.F.; Surroop, D.; Mohee, R. Torrefaction of biomass and plastic from municipal solid waste streams and their blends: Evaluation of interactive effects. *Fuel* **2020**, *277*, 118089. [[CrossRef](#)]
49. Chen, D.; Cen, K.; Cao, X.; Chen, F.; Zhang, J.; Zhou, J. Insight into a new phenolic-leaching pretreatment on bamboo pyrolysis: Release characteristics of pyrolytic volatiles, upgradation of three phase products, migration of elements, and energy yield. *Renew. Sustain. Energy Rev.* **2021**, *136*, 110444. [[CrossRef](#)]
50. Lin, Y.-L.; Zheng, N.-Y.; Hsu, C.-H. Torrefaction of fruit peel waste to produce environmentally friendly biofuel. *J. Clean. Prod.* **2021**, *284*, 124676. [[CrossRef](#)]
51. Zhu, H.; Zhang, Y.; Hu, L.; Liao, Q.; Fang, S.; Gao, R. Dynamic Simulation Based on a Simplified Model of 1/3 Coking Coal Molecule and Its Formation Characteristics of Hydration Films. *ACS Omega* **2021**, *6*, 33339–33353. [[CrossRef](#)]
52. Munawar, M.A.; Khoja, A.H.; Naqvi, S.R.; Mehran, M.T.; Hassan, M.; Liaquat, R.; Dawood, U.F. Challenges and opportunities in biomass ash management and its utilization in novel applications. *Renew. Sustain. Energy Rev.* **2021**, *150*, 111451. [[CrossRef](#)]
53. López-González, D.; Fernandez-Lopez, M.; Valverde, J.; Sanchez-Silva, L. Thermogravimetric-mass spectrometric analysis on combustion of lignocellulosic biomass. *Bioresour. Technol.* **2013**, *143*, 562–574. [[CrossRef](#)]
54. Sarwar, A.; Ali, M.; Khoja, A.H.; Nawar, A.; Waqas, A.; Liaquat, R.; Naqvi, S.R.; Asjid, M. Synthesis and characterization of biomass-derived surface-modified activated carbon for enhanced CO₂ adsorption. *J. CO₂ Util.* **2021**, *46*, 101476. [[CrossRef](#)]
55. Darmstadt, H.; Garcia-Perez, M.; Chaala, A.; Cao, N.-Z.; Roy, C. Co-pyrolysis under vacuum of sugar cane bagasse and petroleum residue: Properties of the char and activated char products. *Carbon* **2001**, *39*, 815–825. [[CrossRef](#)]
56. Xu, F.; Yu, J.; Tesso, T.; Dowell, F.; Wang, D. Qualitative and quantitative analysis of lignocellulosic biomass using infrared techniques: A mini-review. *Appl. Energy* **2013**, *104*, 801–809. [[CrossRef](#)]
57. Gierlinger, N.; Goswami, L.; Schmidt, M.; Burgert, I.; Coutand, C.; Rogge, T.; Schwanninger, M. In situ FT-IR microscopic study on enzymatic treatment of poplar wood cross-sections. *Biomacromolecules* **2008**, *9*, 2194–2201. [[CrossRef](#)] [[PubMed](#)]
58. Kondo, T.; Sawatari, C. A Fourier transform infra-red spectroscopic analysis of the character of hydrogen bonds in amorphous cellulose. *Polymer* **1996**, *37*, 393–399. [[CrossRef](#)]
59. Kubo, S.; Kadla, J.F. Hydrogen bonding in lignin: A Fourier transform infrared model compound study. *Biomacromolecules* **2005**, *6*, 2815–2821. [[CrossRef](#)] [[PubMed](#)]
60. Arteaga-Pérez, L.E.; Grandón, H.; Flores, M.; Segura, C.; Kelley, S.S. Steam torrefaction of *Eucalyptus globulus* for producing black pellets: A pilot-scale experience. *Bioresour. Technol.* **2017**, *238*, 194–204. [[CrossRef](#)]
61. Chen, D.; Cen, K.; Cao, X.; Li, Y.; Zhang, Y.; Ma, H. Restudy on torrefaction of corn stalk from the point of view of deoxygenation and decarbonization. *J. Anal. Appl. Pyrolysis* **2018**, *135*, 85–93. [[CrossRef](#)]
62. Hidayat, W.; Rubiyanti, T.; Sulistio, Y.; Iryani, D.A.; Haryanto, A.; Amrul, A.; Yoo, J.; Kim, S.; Lee, S.; Hasanudin, U. Effects of Torrefaction Using COMB Dryer/Pyrolizer on the Properties of Rubberwood (*Hevea brasiliensis*) and Jabon (*Anthocephalus cadamba*) Pellets. 2021. Available online: <http://repository.lppm.unila.ac.id/id/eprint/32920> (accessed on 5 October 2022).

63. Cheong, K.Y.; Kong, S.H.; Liew, R.K.; Wong, C.C.; Wong, C.S.; Ngu, H.J.; Yek, P.N.Y. Integration of microwave co-torrefaction with helical lift for pellet fuel production. *Green Process. Synth.* **2022**, *11*, 404–410. [[CrossRef](#)]
64. Chen, W.-H.; Kuo, P.-C.; Liu, S.-H.; Wu, W. Thermal characterization of oil palm fiber and eucalyptus in torrefaction. *Energy* **2014**, *71*, 40–48. [[CrossRef](#)]
65. Khan, S.R.; Zeeshan, M.; Masood, A. Enhancement of hydrocarbons production through co-pyrolysis of acid-treated biomass and waste tire in a fixed bed reactor. *Waste Manag.* **2020**, *106*, 21–31. [[CrossRef](#)] [[PubMed](#)]
66. Motasemi, F.; Afzal, M.T. A review on the microwave-assisted pyrolysis technique. *Renew. Sustain. Energy Rev.* **2013**, *28*, 317–330. [[CrossRef](#)]
67. Huang, Y.-F.; Sung, H.-T.; Chiueh, P.-T.; Lo, S.-L. Co-torrefaction of sewage sludge and leucaena by using microwave heating. *Energy* **2016**, *116*, 1–7. [[CrossRef](#)]
68. Huang, Y.-F.; Sung, H.-T.; Chiueh, P.-T.; Lo, S.-L. Microwave torrefaction of sewage sludge and leucaena. *J. Taiwan Inst. Chem. Eng.* **2017**, *70*, 236–243. [[CrossRef](#)]
69. Tian, H.; Jiao, H.; Cai, J.; Wang, J.; Yang, Y.; Bridgwater, A.V. Co-pyrolysis of Miscanthus Sacchariflorus and coals: A systematic study on the synergies in thermal decomposition, kinetics and vapour phase products. *Fuel* **2020**, *262*, 116603. [[CrossRef](#)]
70. Assad Munawar, M.; Hussain Khoja, A.; Hassan, M.; Liaquat, R.; Raza Naqvi, S.; Taqi Mehran, M.; Abdullah, A.; Saleem, F. Biomass ash characterization, fusion analysis and its application in catalytic decomposition of methane. *Fuel* **2021**, *285*, 119107. [[CrossRef](#)]
71. Raza, J.; Khoja, A.H.; Naqvi, S.R.; Mehran, M.T.; Shakir, S.; Liaquat, R.; Tahir, M.; Ali, G. Methane decomposition for hydrogen production over biomass fly ash-based CeO₂ nanowires promoted cobalt catalyst. *J. Environ. Chem. Eng.* **2021**, *9*, 105816. [[CrossRef](#)]
72. Tang, B.; Feng, X.; Huang, S.; Bin, L.; Fu, F.; Yang, K. Variation in rheological characteristics and microcosmic composition of the sewage sludge after microwave irradiation. *J. Clean. Prod.* **2017**, *148*, 537–544. [[CrossRef](#)]
73. Basu, P. *Biomass Gasification, Pyrolysis and Torrefaction: Practical Design and Theory*; Academic Press: Cambridge, MA, USA, 2018.
74. Mehdi, R.; Raza, N.; Naqvi, S.R.; Khoja, A.H.; Mehran, M.T.; Farooq, M.; Tran, K.-Q. A comparative assessment of solid fuel pellets production from torrefied agro-residues and their blends. *J. Anal. Appl. Pyrolysis* **2021**, *156*, 105125. [[CrossRef](#)]
75. Cao, Y.; He, M.; Dutta, S.; Luo, G.; Zhang, S.; Tsang, D.C. Hydrothermal carbonization and liquefaction for sustainable production of hydrochar and aromatics. *Renew. Sustain. Energy Rev.* **2021**, *152*, 111722. [[CrossRef](#)]
76. Feng, Y.; Qiu, K.; Zhang, Z.; Li, C.; Rahman, M.M.; Cai, J. Distributed activation energy model for lignocellulosic biomass torrefaction kinetics with combined heating program. *Energy* **2022**, *239*, 122228. [[CrossRef](#)]
77. Colantoni, A.; Paris, E.; Bianchini, L.; Ferri, S.; Marcantonio, V.; Carnevale, M.; Palma, A.; Civitarese, V.; Gallucci, F. Spent coffee ground characterization, pelletization test and emissions assessment in the combustion process. *Sci. Rep.* **2021**, *11*, 5119. [[CrossRef](#)] [[PubMed](#)]
78. Tumuluru, J.S.; Ghiasi, B.; Soelberg, N.R.; Sokhansanj, S. Biomass Torrefaction Process, Product Properties, Reactor Types, and Moving Bed Reactor Design Concepts. *Front. Energy Res.* **2021**, *462*, 728140. [[CrossRef](#)]
79. Shagali, A.A.; Hu, S.; Li, H.; Chi, H.; Qing, H.; Xu, J.; Jiang, L.; Wang, Y.; Su, S.; Xiang, J. Thermal behavior, synergistic effect and thermodynamic parameter evaluations of biomass/plastics co-pyrolysis in a concentrating photothermal TGA. *Fuel* **2023**, *331*, 125724. [[CrossRef](#)]
80. Brachi, P.; Chirone, R.; Miccio, M.; Ruoppolo, G. Fluidized bed torrefaction of biomass pellets: A comparison between oxidative and inert atmosphere. *Powder Technol.* **2019**, *357*, 97–107. [[CrossRef](#)]
81. Pitsukha, E.; Teplitskii, Y.S.; Buchilko, É. Characteristic Features of Fluidization of Bidisperse Beds in Suffusion Conditions. *J. Eng. Phys. Thermophys.* **2017**, *90*, 1379–1385. [[CrossRef](#)]
82. Teplitskii, Y.; Kovenskii, V. Velocity of full fluidization of a bed of polydisperse granular materials. *J. Eng. Phys. Thermophys.* **2009**, *82*, 291–295. [[CrossRef](#)]
83. Saleem, F.; Abbas, A.; Rehman, A.; Khoja, A.H.; Naqvi, S.R.; Arshad, M.Y.; Zhang, K.; Harvey, A. Decomposition of benzene as a biomass gasification tar in CH₄ carrier gas using non-thermal plasma: Parametric and kinetic study. *J. Energy Inst.* **2022**, *102*, 190–195. [[CrossRef](#)]
84. Is'yomin, R.; Kuz'min, S.; Mikhalyov, A.; Milovanov, O.Y.; Klimov, D.; Nebyvaev, A.; Khaskhachikh, V. Fluidization of a Multicomponent Bed in a Reactor for Co-Torrefaction of Waste Coal and Biomass. *J. Eng. Phys. Thermophys.* **2020**, *93*, 750–756. [[CrossRef](#)]
85. Foong, S.Y.; Liew, R.K.; Yang, Y.; Cheng, Y.W.; Yek, P.N.Y.; Wan Mahari, W.A.; Lee, X.Y.; Han, C.S.; Vo, D.-V.N.; Van Le, Q.; et al. Valorization of biomass waste to engineered activated biochar by microwave pyrolysis: Progress, challenges, and future directions. *Chem. Eng. J.* **2020**, *389*, 124401. [[CrossRef](#)]
86. Yek, P.N.Y.; Cheng, Y.W.; Liew, R.K.; Wan Mahari, W.A.; Ong, H.C.; Chen, W.-H.; Peng, W.; Park, Y.-K.; Sonne, C.; Kong, S.H.; et al. Progress in the torrefaction technology for upgrading oil palm wastes to energy-dense biochar: A review. *Renew. Sustain. Energy Rev.* **2021**, *151*, 111645. [[CrossRef](#)]
87. Chen, C.Y.; Chen, W.-H.; Lim, S.; Ong, H.C.; Ubando, A.T. Synergistic interaction and biochar improvement over co-torrefaction of intermediate waste epoxy resins and fir. *Environ. Technol. Innov.* **2020**, *21*, 101218. [[CrossRef](#)]
88. Chen, X.; Hou, J.; Gu, Q.; Wang, Q.; Gao, J.; Sun, J.; Fang, Q. A non-bisphenol-A epoxy resin with high Tg derived from the bio-based protocatechuic Acid: Synthesis and properties. *Polymer* **2020**, *195*, 122443. [[CrossRef](#)]

89. Szufa, S.; Adrian, Ł.; Piersa, P.; Romanowska-Duda, Z.; Marczak, M.; Ratajczyk-Szufa, J. Torrefaction process of millet and cane using batch reactor. In *Renewable Energy Sources: Engineering, Technology, Innovation*; Springer: Cham, Switzerland, 2020; pp. 371–379.
90. Fan, Y.; Tippayawong, N.; Wei, G.; Huang, Z.; Zhao, K.; Jiang, L.; Zheng, A.; Zhao, Z.; Li, H. Minimizing tar formation whilst enhancing syngas production by integrating biomass torrefaction pretreatment with chemical looping gasification. *Appl. Energy* **2020**, *260*, 114315. [[CrossRef](#)]
91. Huang, C.-L.; Bao, L.-J.; Luo, P.; Wang, Z.-Y.; Li, S.-M.; Zeng, E.Y. Potential health risk for residents around a typical e-waste recycling zone via inhalation of size-fractionated particle-bound heavy metals. *J. Hazard. Mater.* **2016**, *317*, 449–456. [[CrossRef](#)] [[PubMed](#)]
92. Prins, M.J.; Ptasinski, K.J.; Janssen, F.J.J.G. More efficient biomass gasification via torrefaction. *Energy* **2006**, *31*, 3458–3470. [[CrossRef](#)]
93. Chih, Y.-K.; Chen, W.-H.; Tran, K.-Q. Hydrogen production from methanol partial oxidation through the catalyst prepared using torrefaction liquid products. *Fuel* **2020**, *279*, 118419. [[CrossRef](#)]
94. Hashmi, S.; Taqvi, S.A.A.; Abideen, Z.; Ahmed, J.P.; Talha, M.; Bhatti, M.A.; Shahid, H.; Naqvi, S.R.; Almomani, F. Simulation of steam gasification of halophyte biomass for syngas production using Aspen Plus®. *Biomass Convers. Biorefinery* **2022**. [[CrossRef](#)]
95. Chen, W.-H.; Lu, K.-M.; Lee, W.-J.; Liu, S.-H.; Lin, T.-C. Non-oxidative and oxidative torrefaction characterization and SEM observations of fibrous and ligneous biomass. *Appl. Energy* **2014**, *114*, 104–113. [[CrossRef](#)]
96. Shalini, S.; Joseph, K.; Yan, B.; Karthikeyan, O.; Palanivelu, K.; Ramachandran, A. Solid Waste Management Practices in India and China: Sustainability Issues and Opportunities. In *Waste Management Policies and Practices in BRICS Nations*; CRC Press: Boca Raton, FL, USA, 2021; pp. 73–114.
97. Ihsanullah, I.; Khan, M.T.; Zubair, M.; Bilal, M.; Sajid, M. Removal of pharmaceuticals from water using sewage sludge-derived biochar: A review. *Chemosphere* **2022**, *289*, 133196. [[CrossRef](#)]
98. Huang, Y.-F.; Chiueh, P.-T.; Kuan, W.-H.; Lo, S.-L. Effects of lignocellulosic composition and microwave power level on the gaseous product of microwave pyrolysis. *Energy* **2015**, *89*, 974–981. [[CrossRef](#)]
99. Matsumura, Y.; Minowa, T.; Potic, B.; Kersten, S.R.; Prins, W.; van Swaaij, W.P.; van de Beld, B.; Elliott, D.C.; Neuenschwander, G.G.; Kruse, A. Biomass gasification in near-and super-critical water: Status and prospects. *Biomass Bioenergy* **2005**, *29*, 269–292. [[CrossRef](#)]
100. Couhert, C.; Salvador, S.; Commandre, J.-M. Impact of torrefaction on syngas production from wood. *Fuel* **2009**, *88*, 2286–2290. [[CrossRef](#)]
101. Deng, J.; Wang, G.-j.; Kuang, J.-h.; Zhang, Y.-l.; Luo, Y.-H. Pretreatment of agricultural residues for co-gasification via torrefaction. *J. Anal. Appl. Pyrolysis* **2009**, *86*, 331–337. [[CrossRef](#)]
102. van der Stelt, M.J.C.; Gerhauser, H.; Kiel, J.H.A.; Ptasinski, K.J. Biomass upgrading by torrefaction for the production of biofuels: A review. *Biomass Bioenergy* **2011**, *35*, 3748–3762. [[CrossRef](#)]
103. Felix, C.B.; Ubando, A.T.; Chen, W.-H.; Goodarzi, V.; Ashokkumar, V. COVID-19 and industrial waste mitigation via thermochemical technologies towards a circular economy: A state-of-the-art review. *J. Hazard. Mater.* **2022**, *423*, 127215. [[CrossRef](#)]
104. Ubando, A.T.; Felix, C.B.; Chen, W.-H. Biorefineries in circular bioeconomy: A comprehensive review. *Bioresour. Technol.* **2020**, *299*, 122585. [[CrossRef](#)]
105. Qayimova, Z. Prospects for the development of Islamic banking services market in commercial banks of Uzbekistan. *Центр Научных Публикаций (buxdu.uz)* **2021**, *7*.
106. Singh, R.P.; Tyagi, V.V.; Allen, T.; Ibrahim, M.H.; Kothari, R. An overview for exploring the possibilities of energy generation from municipal solid waste (MSW) in Indian scenario. *Renew. Sustain. Energy Rev.* **2011**, *15*, 4797–4808. [[CrossRef](#)]
107. Corrado, S.; Sala, S. Bio-economy contribution to circular economy. In *Designing Sustainable Technologies, Products and Policies*; Springer: Cham, Switzerland, 2018; pp. 49–59.